PHYSICAL AND FUNCTIONAL CHARACTERIZATION OF ACTIVE FISH GELATIN FILMS INCORPORATED WITH LIGNIN

R. NÚÑEZ-FLORES, B. GIMÉNEZ, F. FERNÁNDEZ-MARTÍN, M.E. LÓPEZ-CABALLERO, M.P. MONTERO & M. C. GÓMEZ-GUILLÉN*

Instituto de Ciencia y Tecnología de Alimentos y Nutrición (ICTAN-CSIC).

C/ José Antonio Novais, 28040 – Madrid (Spain)

* Corresponding author. Tel: +34-31-5492300; fax: +34-91-5493627.

E-mail address: cgomez@ictan.csic.es

ABSTRACT

In order to provide gelatin films with antioxidant capacity, two sulphur-free water-insoluble lignin powders (L_{1000} and L_{2400}) were blended with a commercial fish-skin gelatin from warm water species at a rate of 85% gelatin: 15% lignin (w/w) **(G-L_{1000} and G-L_{2400})**, using a mixture of glycerol and sorbitol as plasticizers. The water soluble fractions of **G-L_{1000} and G-L_{2400}** films were 39.38±1.73 % and 46.52±1.66 % respectively, rendering radical scavenging capacity (2,2'-azino-bis(3-ethylbenzothiazoline-6-sulphonic acid, ABTS assay) of 27.82±2.19 and 15.31±0.88 mg vitamin C equivalents/g film, and ferric ion reducing ability (FRAP assay) of 258.97±8.83 and 180.20±5.71 μmol Fe^{2+} equivalents /g film, respectively. Dynamic oscillatory test on film-forming solutions and Attenuated Total Reflectance (ATR) - FTIR spectroscopy study on films revealed strong lignin-induced protein conformational changes, producing a noticeable plasticizing effect on composite films, as deduced from the study of mechanical (traction and puncture tests) and thermal properties (Differential Scanning Calorimetry, DSC). The gelatin films lose their typical transparent and colourless appearance by blending with lignin; however, the resulting composite films gained in light barrier properties, which could be of interest in certain food applications for preventing ultraviolet-induced lipid oxidation. Lignin proved to be an efficient antioxidant at non-cytotoxic concentrations, however, no remarkable antimicrobial capacity was found.

Keywords: film, fish gelatin, lignin, physical properties, ATR-FTIR, DSC, antioxidant, cytotoxic, antimicrobial

INTRODUCTION

Gelatin has been one of the most studied biopolymers on account of its film-forming ability and its usefulness as an outer film to protect food from drying and exposure to light and oxygen (Arvanitoyannis, 2002). Fish gelatins exhibit good film-forming properties, yielding transparent, nearly colourless and highly extensible films (Avena-Bustillos et al., 2006; Jongjareonrak, Benjakul, Visessanguan, Prodpran & Tanaka, 2006; Zhang, Wang, Herring & Oh, 2007; Carvalho et al., 2008; Gómez-Estaca, Montero, Fernández-Martín & Gómez-Guillén, 2009). Furthermore, enriching gelatin films with antioxidants and/or antimicrobial substances will extend the functional properties of these biodegradable films and provide an active packaging biomaterial. Because of "clean labelling" concerns, there is growing interest in using natural compounds, such as polyphenolic plant extracts (Gómez-Guillén, Ihl, Bifani, Silva, & Montero, 2007) or α-tocopherol (Jongjareonrak, Benjakul, Visessanguan & Tanaka, 2008) in the formulation of active fish gelatin films.

Lignin, most commonly derived from wood, is largely thrown off as a waste product in pulp and paper industries. It is a complex polydisperse natural polymer made up of phenyl-propane (C6−C3) units that bind cellulose fibres together, thus hardening and strengthening the plant cells. Lignin derivatives have been incorporated as fillers in different synthetic polymer matrices to develop lignin-based materials with improved physical properties (Feldman, Lacasse, & Beznaczuk, 1986; Kadla & Kubo, 2003; Mishra, Mishra, Kaushik, & Khan, 2007; Cui, Xia, Chen, Wei, & Huang, 2007). During the last decade, a great deal of research was devoted to the development of lignin-containing biopolymeric materials, on account of its renewable, non-toxic and biodegradable character (Baumberger, Lapierre, Monties, Lourdin & Colonna, 1997; Chiellini, Cinelli, Fernandes, Kenawy & Lazzeri, 2001; Li, & Sarkanen, 2002; Vengal, & Srikumar, 2005; Ban, Song & Lucia, 2007; Wu, Wang, Li, Li, & Wang, 2009; Julinová et al., 2010). Lignin has been referred to as a plasticizing agent in composite films with

starch (Wu et al., 2009). However, in composites prepared using adipic acid-modified starch microparticles within a corn-starch matrix, addition of lignin produced higher tensile strength and lower elongation capacity (Spiridon, Teaca & Bodirlau, 2011). Similarly, lignin acted as a reinforcing agent with cellulose (Rohella, Sahoo, Paul, Choudhury & Chakravortty, 1996) or polyethylene oxide (Kadla & Kubo, 2003), in all cases providing adequate miscibility with the polymer. In addition, the incorporation of small amounts of lignin into polypropylene films has been shown to stabilize the composite material against photo-oxidation (Kosikova, Demianova & Kakurakova, 1993). The hydrophobic nature of lignin has been also shown to produce strong reduction of water absorbency and transparency in starch-based films (Ban, Song & Lucia, 2007).

Due to their complex polyphenolic nature, lignins can exert antioxidant (radical scavenging capacities) (Lu, Chu & Gau, 1998; Satoh et al., 1999; Dizhbite, Telysheva, Jurkjane, & Viesturs, 2004; Pan, Kadla, Ehara, Gilkes, & Saddler, 2006; Ugartondo, Mitjans, & Vinardell, 2008) and antimicrobial properties (Dong et al., 2011), thus opening up the possibility of new potential applications. As a result of the molecular complexity of lignins, it becomes difficult to assign the antioxidant efficacy to specific structural components, compared to the activities of chemically defined tannins and flavonoids (Sakagami et al., 2005). The radical scavenging activity of lignins is influenced by structural features, such as the presence of phenolic hydroxyl groups, methoxy groups, π-conjugation systems as well as the molecular weight, heterogeneity and polydispersity (Dizhbite et al., 2004). Only a few studies have reported the cytotoxic effects of lignins. A good correlation between cytotoxicity and some features such as carbohydrate content and polydispersity has been reported; the lignins with higher polidispersity and lower carbohydrate content are the most cytotoxic (Ugartondo et al., 2008). Lignin derivatives have been shown to be effective antioxidants at concentrations that are not harmful to normal human cells, thus furthering their possible

use in the formulation of active food packaging biomaterials (Ugartondo et al., 2008; Núñez-Flores et al., 2012). In this sense, the appearance, protein quality and oxidative stability of salmon fillets subjected to high pressure processing were enhanced by the combined use of a gelatin-lignin film similar to the one characterized in the present study (Ojagh, Nuñez-Flores, López-Caballero, Montero & Gómez-Guillén, 2011).

The antimicrobial properties of lignins have been reported previously in the literature, both in model system and in experimental animals, for example, from hydrolysates of several lignocellulosic materials (ethyl acetate extracts) (Cruz et al., 2001), lignin-related structures from alkaline extractions (Oh-Hara et al., 1990), kraft-lignins (Dizhbite et al., 2004) and to a lesser extent from lignosulphonates (Núñez-Flores et al., 2012). The origin of lignin might influence their antimicrobial properties. Thus, Oh-Hara et al. (1990) reported that the antimicrobial activity induced by commercial lignins was much lower than that induced by fractions of pine cone extracts obtained by successive alkaline extractions (and then recovered as acid precipitates at pH 5). By comparing the spectra, these authors found that some pine cone extract include more alkenic double bonds and fewer OCH3 than commercial alkali-lignin, while a coumaryl type of lignin structure could be responsible for the antimicrobial activity.

The aim of the present work was to produce antioxidant fish gelatin films by mixing gelatin with two types of lignin, and to characterize structural, mechanical, optical, and thermal properties of the composite active material. In order to establish the harmlessness and potential functionality in food packaging applications, cytotoxicity, radical scavenging capacity and antimicrobial capacity of lignin were also tested.

MATERIALS & METHODS

Materials

Commercial type A warm-water fish gelatin was supplied by Rousselot S.A.S. (Puteaux, France). For comparison purposes, two sulphur-free water-insoluble commercial lignin powders were used: Protobind 2400 (L_{2400}) and Protobind 1000 (L_{1000}) (Granit Recherche & Developpement SA, Lausanne, Switzerland). According to manufacturer's specifications, both lignins aqueous suspensions presented pH~4, number average molecular weight ~1000 Da and particle size < 210 micron, differing in bulk density (~0.55 kg/L in L_{2400} *vs* ~0.30 kg/L in L_{1000}) and in softening temperature (~130ºC in L_{2400} *vs* ~200 ºC in L_{1000}). Glycerol and sorbitol were obtained from Panreac (Barcelona, Spain). All other reagents used were of analytical grade. The 2,4,6-tripyridyl-s-triazine, the 2,2-azino-bis-(3-ethylbenzothiazoline-6-sulfonic acid) (ABTS) radical, Vitamin C and the 1,1-Diphenyl-2-picrylhydrazyl (DPPH) radical were purchased from Sigma-Aldrich (St. Louis, MO, USA). The MTS (3-(4,5-dimethylthiazol-2-yl)-5-(3-carboxymethoxyphenyl)-2-(4-sulfophenyl)-2H-tetrazolium) salt was supplied by Promega Biotech Ibérica (Madrid, Spain).

Preparation of films

The gelatin-lignin film forming solution (FFS) was prepared by dissolving the fish gelatin in distilled water (3.4 % w/v) at 40 ºC, adding sorbitol (15 g/100 g gelatin) and glycerol (15 g/100 g gelatin) as plasticizers. The lignin powder was added to a final concentration of 0.6% w/v in the FFS. This concentration was selected according to previous experiments. The mixture was stirred at 40 ºC for 15 min and was alkalinized to ~pH=11 to obtain a good blend with total solubility. The films were made by casting an amount of 40 ml over a plate of 12x12 cm^2 and drying at 45 ºC in a forced-air oven for 15 h to yield a uniform thickness of ~100 ± 10 µm. Films were conditioned over a saturated solution of KBr in desiccators for 4 d.

144 **Viscoelastic properties of film forming solutions**

145 Dynamic oscillatory study of the film-forming solutions was carried out on a Bohlin
146 CVO-100 rheometer (Bohlin Instruments Ltd., Gloucestershire, UK) using a cone-plate
147 geometry (cone angle 4º, gap 0.15 mm). Cooling and heating from 30 to 2 ºC and back
148 to 30 ºC took place at a scan rate of 1 ºC/min, a frequency of 0.5 Hz, and a target strain
149 of 0.5%. The elastic modulus (G'; Pa), viscous modulus (G''; Pa) and phase angle (º)
150 were plotted as functions of temperature in the heating ramp from 2 to 30ºC. At least
151 two determinations were performed for each sample. The experimental error was less
152 than 6% in all cases.

153

154 **Film thickness**

155 Film thickness was measured using a digital micrometer (Mitutoyo, model MDC-25M,
156 Kanagawa, Japan), averaging nine different locations.

157

158 **Mechanical properties**

159 Tensile strength (TS) and elongation at break (EAB) of the films were determined using
160 a TA.XT.plus Texture analyser (SMS, Surrey, UK). The samples were cut into
161 rectangles (20 mm width and 50 mm length), fixed on the grips of the device with a gap
162 of 20 mm, and tractioned at a speed of 1 mm/s. Results of TS and EAB were average
163 of five determinations, and expressed as N/m^2 and %, respectively.

164 A puncture test was performed to determine the breaking force and the breaking
165 deformation of the films. Films were placed in a cell 5.6 cm in diameter and punched to
166 the breaking point using the same texture analyser, with a round-ended stainless-steel
167 plunger 3 mm in diameter at a cross-head speed of 60 mm/min. Breaking force was
168 expressed in N and breaking deformation in %, according to Sobral, Menegalli,

169 Hubinger & Roques (2001). All determinations are the means of at least five
170 measurements.

171

172 **Water solubility**

173 Water solubility was measured using the same methodology as described by Núñez-
174 Flores et al. (2012). Film solubility was calculated by the equation FS (%) = ((Wo-
175 Wf)/Wo)•100, where Wo was the initial weight of the film expressed as dry matter and
176 Wf was the weight of the undissolved desiccated film residue. All tests were carried out
177 in triplicate.

178

179 **Water activity (A_w)**

180 Water activity (A_w) of films was measured using a portable LabMaster-a_w (Novasina,
181 Lachen, Switzerland) instrument. Values were recorded at equilibrium when a_w of any
182 two readings were <0.001 at constant temperature (25 °C). Measurements were done
183 at least in triplicate.

184

185 **Water vapour permeability**

186 Water vapour permeability (WVP) was determined following a gravimetric method as
187 described below. Films were attached over the openings of cells (permeation area =
188 15.9 cm^2) containing desiccated silica gel, and the cells were placed in desiccators with
189 distilled water at 22 ºC. The cells were weighed every hour for at least 6 h. Water
190 vapour permeability was calculated using the equation $WVP = w \cdot x \cdot t^{-1} \cdot A^{-1} \cdot \Delta P^{-1}$, where w
191 was weight gain (g), x film thickness (mm), t elapsed time for the weight gain (h), and
192 ΔP the partial vapour pressure difference between the dry atmosphere and pure water

(2642 Pa at 22 ºC). Results have been expressed as g•mm•h^{-1}•cm^{-2}•Pa^{-1}. All tests were carried out at least in triplicate.

Light barrier properties

The films were cut into a rectangle piece and directly placed against one side of a UV-1601 spectrophotometer (Model CPS-240, Shimadzu, Kyoto, Japan) test cell, using an empty test cell as the reference. The light barrier properties of films were measured by exposing the films to light absorption at wavelengths ranging from 690 nm to 200 nm. The opacity of the films was calculated by the equation $O=Abs_{600}/x$, where Abs_{600} is the value of absorbance at 600 nm and x is the film thickness in mm. Measurements were done at least in triplicate.

Colour measurements

The colour parameters Lightness, Redness and Yellowness were measured in the *L**, *a**, *b** mode of CIE scale using a Konica Minolta 3500-D colorimeter (Osaka, Japan). Results are average of at least 10 replicates. Hue angle (h^*_{ab}) and Chroma (C^*_{ab}) values were calculated using the following equations:

$$h^*_{ab} = \tan^{-1}(b^*/a^*), \text{ when } [+a^*,+b^*]$$

$$h^*_{ab} = 180 + \tan^{-1}(b^*/a^*), \text{ when } [-a^*,-b^*]$$

$$h^*_{ab} = 360 + \tan^{-1}(b^*/a^*), \text{ when } [+a^*,-b^*]$$

$$C^*_{ab} = (a^{*2} + b^{*2})^{1/2}$$

Attenuated Total Reflectance (ATR) - FTIR spectroscopy

Infrared spectra between 4000 and 650 cm^{-1} were recorded using a Perkin Elmer Spectrum 400 Infrared Spectrometer (Perkin Elmer Inc, Waltham, MA, USA) equipped with an ATR prism crystal accessory, as reported previously (Núñez-Flores et al., 2012). All experiments were performed at least in triplicate and represented as average spectra.

Differential Scanning Calorimetry (DSC)

Calorimetric analysis was performed using a model TA-Q1000 differential scanning calorimeter (TA Instruments, New Castle, DE, USA) previously calibrated by running high purity indium. Samples of approximately 10 mg (± 0.002 mg) were weighed out using a model ME235S electronic balance (Sartorious, Goettingen, Germany) and were tightly encapsulated in hermetic aluminum pans and scanned under dry nitrogen purge (50 mL/min). An empty hermetic aluminum pan was used as reference. Freshly conditioned films were cooled to − 80 ºC, or 0 ºC, at 10 ºC/min and scanned up to 90 ºC at a heating rate of 10 ºC/min. After cooling at the same rate down to the corresponding initial temperature, a second heating scan was run. Glass transition temperatures, Tg (ºC), were calculated by the inflection-midpoint method and usually reported on the first heating scans, in order to thermally characterize the same material used in the rest of analyses. Tg as well as melting transition data (Temperature, Tm; Enthalpy change, ΔH) were reported as mean values with their standard deviations of at least triplicate samples for each film. The energetic parameter was normalized to dry matter content of the corresponding film sample, ΔH (J/gdm), which needed from the desiccation (105 ºC, pin hole in the lid) of each individual capsule content.

Cryoscanning electron microscopy (Cryo-SEM)

241 Cryoscanning electron microscopy (Cryo-SEM) was used to examine microstructural
242 representative cross sections of films. Samples were mounted with OCT compound
243 (Gurr) and mechanically fixed onto the specimen holder using the Oxford CT1500
244 Cryosample Preparation Unit (Oxford Instruments, Oxford, England). Samples were
245 frozen in subcooled liquid nitrogen for 2 min and then transferred to the preparation
246 unit. After ice sublimation, the surfaces were gold sputter coated, and subsequently
247 transferred into the cold stage of the SEM chamber. Specimens were observed with a
248 DSM960 Zeiss SEM microscope (Zeiss, Oberkochen, Germany) at -135 ºC under a 15
249 kV acceleration potential.

250

251 **Antioxidant properties of films**

252 The ferric ion reducing capacity (FRAP) and the radical scavenging ability (ABTS)
253 assays were used to measure the antioxidant activity of the films. An aliquot of the
254 filtrate obtained from the determination of the film water solubility was employed as the
255 sample. The method used for the FRAP and ABTS assays was previously described by
256 Gómez-Estaca et al. (2009). The results were expressed as μmol Fe^{2+} equivalents per
257 g of film for FRAP and mg of Vitamin C Equivalent Antioxidant Capacity (VCEAC) per g
258 of film for ABTS, based on standard curves of $FeSO_4 \cdot 7H_2O$ and vitamin C, respectively.

259

260 **Antioxidant activity of lignin**

261 The antioxidant activity of lignin (L_{1000}) was determined based on the 1,1-Diphenyl-2-
262 picrylhydrazyl (DPPH) radical scavenging ability. The assay was carried out as
263 described by Brand-Williams, Cuvelier, and Berset (1995) with some modifications
264 (Fukumoto & Mazza, 2000). L_{1000} was analyzed by triplicate testing at least five different
265 concentrations ranging from 7 to 250 μg/ml. The radical scavenging activity was

266 expressed as IC_{50} value, the concentration necessary to quench 50% of initial DPPH
267 radical. The percentage of scavenged DPPH was plotted versus the concentration of
268 L_{1000}, and that required to quench 50% of initial DPPH radical was obtained from the
269 graph by linear regression. Trolox (6-hydroxy-2, 5, 7, 8-tetramethylchroman-2-
270 carboxylic acid), a water-soluble vitamin E analogue, was used as reference
271 compound. The DPPH radical scavenging capacity of Trolox, expressed as IC_{50} value,
272 was determined by testing concentrations ranging from 3 to 50 μg/ml.

273

274 **Cytotoxic effect of lignin**

275 *Culture of cell lines*

276 The mouse fibroblast cell line 3T3-L1 was grown in DMEM medium (4.5 g/L glucose)
277 supplemented with 10% foetal bovine serum (FBS), at 37 ºC under a humidified 5%
278 CO_2 atmosphere. When the cells were approximately 70% confluent, they were split by
279 mild trypsinization and seeded into 24-well plates at a density of 1 x 10^4 cells/well. The
280 24-well plates were incubated at 37 ºC and 5% CO_2 for 24 h. Runs were performed in
281 triplicate with different passage cells.

282 *Experimental treatments*

283 After 1 day of incubation, cultures were exposed to increasing concentrations of lignin
284 (L_{1000}) sterilized by filtration and diluted in DMEM medium supplemented with 10%
285 FBS. Controls (containing only the culture medium) were included in each plate. The
286 plates were incubated at 37 ºC with 5% CO_2 for 24 h.

287 *MTS assay*

288 The viability of the 3T3-L1 cells treated with increasing concentrations of LS for 24 h
289 was determined by the MTS assay, composed of the tetrazolium salt MTS (3-(4,5-

290 dimethylthiazol-2-yl)-5-(3-carboxymethoxyphenyl)-2-(4-sulfophenyl)-2H-tetrazolium)
291 and an electron coupling reagent (PMS, phenazine methosulfate). This assay is based
292 on the conversion of the tetrazoliumcompound into a coloured, aqueous soluble
293 formazan product by mitochondrial activity of viable cells at 37 ºC. The amount of
294 formazan produced by dehydrogenase enzymes is directly proportional to the number
295 of living cells in culture. MTS and PMS were combined in a ratio of 20:1 and the
296 mixture was added to the culture medium in a ratio of 1:5 (reagent mixture:culture
297 medium). Cells were washed with PBS and the medium containing MTS/PMS was
298 added (500 ml per well). After 1 h of further incubation, the absorbance was measured
299 in a microplate reader at 485 nm (Appliskan, Thermo Scientific, Madrid, Spain).

300

301 **Antimicrobial capacity of lignin**

302 The antimicrobial activity of lignin was determined by the disk diffusion method in agar
303 against 26 microbial strains (including Gram-positive and Gram-negative bacteria,
304 yeast and molds) as previously described (Núñez-Flores et al., 2012). Each
305 determination was performed in triplicate.

306

307 **Statistical analysis**

308 Statistical tests were performed using the SPSS computer program (SPSS Statistical
309 Software Inc., Chicago, IL, USA). One-way analysis of variance was carried out.
310 Differences between pairs of means were assessed on the basis of confidence
311 intervals using the Duncan test. The level of significance was $p < 0.05$.

312

313 **RESULTS & DISCUSSION**

Physical properties of films

Table 1 shows the physical properties of gelatin and gelatin-lignin (G-L) composite films. The addition of lignin produced an evident plasticizing effect, as deduced from significant decreases in both tensile strength (TS) and breaking force (BF) in the composite films, together with a marked increase in elongation at break (EAB) as well as in breaking deformation (BD). The composite films were highly stretchable, with percent elongation values similar to those reported previously by Vengal and Srikumar (2005) in gelatin-lignin films, and comparable to the highly extensible gelatin films obtained from the skin of cold water fish species (Carvalho et al., 2008; Pérez-Mateos et al., 2009). The films containing lignin L_{2400}, which was characterized by a higher bulk density and a lower softening point than lignin L_{1000}, were characterized by significantly ($p<0.05$) lower TS values than G-L_{1000} films. The reduced TS in the gelatin-lignin composite films was related to an increased water activity, which was more pronounced in G-L_{2400} film. Thus, the apparent plasticizing effect observed in composite films could be attributed not only to a direct effect of lignin but also to the presence of water free molecules**, causing a reduction in intermolecular attractive forces between polymer chains** (Cuq, Gontard, Cuq & Guilbert, 1997). Lignin has provided adequate miscibility with different polymers. It has been reported as a plasticizing agent in composite films with starch (Baumberger et al., 1997; Wu et al., 2009) or with soy protein isolate (SPI) (Huang, Zhang & Chen, 2003), but in the latter case only when incorporated at moderate concentrations (from 10 to 20 parts). In contrast, lignin acts as a reinforcing agent with cellulose (Rohella et al., 1996) or polyethylene oxide (Kadla & Kubo, 2003). A significant increase in TS has been also reported for SPI-lignin blends (Huang et al., 2003). However, it should be noted that SPI films were considerably less resistant than the gelatin films obtained in this study, in accordance to a previous work performed by Cao et al. (2007).

Regarding film water barrier properties, the water solubility was slightly but significantly ($p<0.05$) reduced only in the G-L_{1000} film. To this respect, it should be taken into account that the solubility of the control gelatin film (~ 44%) was relatively low, especially when compared to extremely high water-soluble films prepared with gelatins from cold-water species, such as cod (Pérez-Mateos et al., 2009) or halibut (Carvalho et al., 2008). In a previous work, the water solubility of films made of cold-water fish skin gelatin with added lignosulphonate was considerably reduced from 92.50% in the control gelatin film to 54.54% in the blend film (Núñez-Flores et al., 2012). Regarding water vapor permeability (WVP), lignin L_{1000} did not induce any significant change when compared to the control gelatin film; however WVP was considerably increased by the L_{2400} lignin, coinciding with a greater water-induced plasticization effect which made the polymer network less dense and thus more permeable, in agreement with Cuq et al. (1997).

Light barrier properties

Both types of lignin conferred a dark brown reddish colour leading to a noticeable reduction in lightness of the gelatin composite films (Table 2). G-L_{2400} film was characterized by a slightly higher tendency to both redness (a* value) and yellowness (b* value), as compared to the G-L_{1000} film. The gelatin-lignin films showed marked differences both in hue angle (h^*_{ab}) (358.99±0.33 for G-L_{1000} and 1.73±0.19 for G-L_{2400}) and chroma (C^*_{ab}) values (0.59±0.07 for G-L_{1000} and 2.24±0.25 for G-L_{2400}). Thus, G-L_{2400} film was characterized by a more intense brownish coloration than G-L_{1000} film. Furthermore, both composite films were noticeably different from the gelatin film (h^*_{ab} = 179.94±0.16; C^*_{ab} = 1.05±0.00), which was visually almost colourless. As shown in Table 2, the addition of lignin increased greatly the opacity of gelatin composite films, especially with L_{1000} lignin. Thus, the gelatin films lose their typical transparent and

366 colorless appearance by blending with lignin. However, the resulting composite films
367 gained in light barrier properties, which could be of interest in certain food applications
368 for preventing UV-induced lipid oxidation. Figure 1 shows the spectroscopic scanning
369 of the films at wavelengths between 700 and 250 nm. Both types of composite films
370 showed a pronounced increase in the absorbance level within the UV region as
371 compared to the gelatin films, approximately 35-fold higher at wavelengths in the range
372 of 400-300 nm and 5.5-fold higher below 280 nm. From 400 nm upwards, G-L_{1000} film
373 had higher light absorbance than G-L_{2400}, in agreement with differences in the
374 transparency level. The chromophoric nature of lignin is known to be highly capable of
375 protecting against UV radiation (Ban, Song & Lucia, 2007; Pereira et al., 2007). In
376 addition, lignin has been also reported to act as a potent UV absorber in lignin-PVC
377 blend films (Mishra et al., 2007).

378

379 **Viscoelastic properties of film forming solutions**

380 The viscoelastic behavior of film forming solutions containing either gelatin or gelatin-
381 lignin blend was studied by cooling down from 30 to 5 °C and heating back to 30 °C, in
382 order to determine the degree of interference of both types of lignin in the arrangement
383 of gelatin polypeptide chains into cold-induced triple helical structure to form a gel.
384 Viscoelastic parameters (elastic modulus *G'*, viscous modulus *G''* and phase angle)
385 registered at 5 ºC, as well as gelling (Tg) and melting (Tm) temperatures, are shown in
386 Table 3. The partial replacement of gelatin by lignin strongly reduced the gelling
387 capacity of gelatin, as deduced from the pronounced drop in G' and G'', with an
388 associated increase in phase angle, at the end of the cooling ramp. Moreover, the
389 marked down-shift of both gelling and melting temperatures in the blend solutions
390 denoted a considerable decrease in thermostability of the formed triple helices by the
391 presence of lignin. Regarding the type of lignin, a greater degree of interference in the

triple helical structure development was evidenced in the G-L_{1000} blend, as clearly deduced from the ~3-fold higher phase angle value in comparison to the G-L_{2400} blend. The lower bulk density of lignin L_{1000} might be a possible reason for the greater interference, by facilitating its interaction with gelatin polypeptide chains.

The observed changes in the dynamic viscoelastic behavior of gelatin film forming solution as a result of lignin addition were similar to those reported for gelatin with added lignosulphonate (Núñez-Flores et al., 2012), but much more pronounced than with poly(vinyl) alcohol (Moraes, Carvalho, Bittante, Solorza-Feria & Sobral, 2009) or different plant aqueous extracts (Gómez-Guillén et al., 2007; Gómez-Estaca, Montero, Fernández-Martín, Alemán, Gómez-Guillén, 2009).

Conformational properties

Figure 2 shows the ATR-FTIR spectra of gelatin and gelatin-lignin films in the range of 3800-900 cm^{-1}. The addition of lignin caused a marked decrease in the intensity of amide A (~3283 cm^{-1}), amide I (~1631 cm^{-1}), amide II (~1543 cm^{-1}) and amide III (~1238 cm^{-1}) bands of gelatin. Besides a slight protein "dilution effect" as a result of partial replacement of gelatin by lignin, such a decrease would be largely attributed to noticeable lignin-induced protein conformational changes, especially attending to differences in amide I band (Surewicz & Mantsch, 1988). The slight frequency up-shift of amide I peaks in the composite films (G: 1631 cm^{-1}; G-L_{1000}: 1635 cm^{-1}; G-L_{2400}: 1635 cm^{-1}), would indicate an eventual disruption of hydrogen bonding at the C=O groups of gelatin polypeptides by the lignin interference, regardless the lignin type. In this connection, addition of lignin has been also shown to prevent interaction among SPI molecules in SPI-lignin blend films (Huang et al., 2003). Infrared absorption of lignin carbonyl groups, which has been described at higher wavenumbers (~ 1740-1700 cm^{-1}) (Fernandes, Winkler, Job, Radovanocic, & Pineda, 2006, Mishra et al., 2007, Pereira

et al., 2007) were not detectable in the spectra of the gelatin-lignin films. On the other hand, FTIR spectra confirmed the higher protein hydration level in the G-L_{2400} film, in comparison to G-L_{1000}, deduced from the slightly higher intensity of amide A band and the frequency up-shift of amide II peak (1544 cm^{-1} *vs* 1539 cm^{-1}) in those films (Yakimets et al., 2005).

The prominent band at ~1035 cm^{-1} in the gelatin films could be largely attributed to the interactions arising between plasticizers (C-O stretch of glycerol and sorbitol) and film structure (Bergo and Sobral, 2007; Hoque, Benjakul, & Prodpran, 2011). Despite the film plasticizing effect caused by lignin, no evident changes at this level were observed in the gelatin-lignin films, discarding thus remarkable interactions between lignin and plasticizers.

The second derivative of the amide I band, depicted in Fig. 3, revealed noticeable changes induced by the presence of lignin in the composite films, as denoted by the reduced intensity of peaks at ~ 1660 cm^{-1}, 1652 cm^{-1} and ~ 1630 cm^{-1}, which had been related, respectively, to the presence of triple helix, single α-helix, and disordered coil structures in gelatin matrices (Payne & Veis, 1988; Prystupa & Donald, 1996). The most pronounced changes in composite films within the range of ~1635-1625 cm^{-1} were indicative of the strong interference caused by both lignins in the hydrogen bonding between water and imide residues (Payne & Veis, 1988). Such an interference, which was also evidenced in the triple helical component at ~ 1660 cm^{-1}, was consistent with the reduced capacity in triple helix development of lignin-containing film forming solutions.

Thermal properties

Typical DSC behavior of films from fish gelatin alone (G) or blended with lignin (G-L) are shown in Fig. 4. Films G exhibited thermal characteristics resembling those

444 reported in a previous publication (Gómez-Estaca et al., 2009) concerning a type A
445 tuna-skin gelatin prepared at the laboratory. Essentially, the thermal behavior of gelatin
446 single films consisted (Trace G, solid line) of a glass transition process with a Tg ~ 18.5
447 ± 0.5 °C, followed by an endothermic event involving a bimodal melting with maximum
448 temperatures Tm at around 61.3 ± 0.5 °C and 79.5 ± 0.5 °C. These thermal data were
449 something higher than corresponding ones of previous work, particularly Tg, which
450 notwithstanding indicated a close similitude between that tuna-skin gelatin and current
451 commercial warm-water fish gelatin. Melting enthalpy ΔH was 11.3 ± 0.41 J/gdm. This
452 kind of complex endothermic melting in G films has also been reported by Rahmann,
453 Al-Saidi & Guizani (2008) and Gómez-Estaca et al. (2009) by additionally using MDSC
454 (Modulated DSC) and tentatively attributed to a normal melting overlapped with a
455 crystal perfection process. Second heating scans (Trace G, dash line) displayed a
456 slightly lower (~ 3 °C) glass transition temperature but associated with a higher (~ 1/3)
457 heat capacity change in the system, at the time that no sign of remnant melting was
458 detected. This may likely be due to a different thermal history of a wholly amorphous
459 and bigger (total) G amount participating in the glass transition process.

460 When the film was conditioned at 0 °C, corresponding glass transition seemed to be
461 only visible by MDSC as reported in a previous work (Gómez-Estaca et al., 2009),
462 probably due to the small of the temperature gap. The melting endotherm (Trace G, dot
463 line) evolved less sharply (rounded peaks) and the main melting temperature was
464 considerably and significantly lower (53.2 ± 2.5 °C) than that at −80 °C, while the
465 second peak remained almost unaltered (80.8 ± 0.3 °C). The melting enthalpy value
466 was 9.57 ± 0.21 J/g_{dm}, also significantly lower (~ 15%) than in the low temperature
467 conditioning. These differences can likely be due to the different thermal crystallization
468 conditioning which yielded a lower amount and a different crystal material. These
469 thermal data were much more similar to those from Gómez-Estaca et al. (2009) than
470 previous ones due to much more similar thermal histories between samples. In

general, current results were not able for comparison with those from others (Badii, & Howell, 2006; Rahmann et al., 2008) on fish gelatin films, because disparity appeared not only among gelatins used but also among the different plasticizers present in the films.

Regarding G-L_{1000} and G-L_{2400} films, a new glass transition process arose at the lowest temperature region (Traces G-L_{1000} and G-L_{2400}, solid lines), with Tg values of – 63.4 ± 0.8 °C and – 54.9 ± 0.6 °C, respectively (Fig. 4). Tg data were significantly lower in G-L_{1000} than in G-L_{2400}, this suggesting a differential plasticization capacity between both lignin types (L_{1000} > L_{2400}). This glass transition process was followed by a second one at the significantly different Tg values of – 23.1 ± 0.4 °C and – 20.6 ± 0.6 °C respectively. Both Tg values were significantly lower than that of G, indicating the plasticization role of lignin (L_{1000} > L_{2400}), as well as an (initially) total miscibility between both types of L and G at the proportions used in the blended films. Corresponding melting endotherms were considerably smaller (with a flatter trace) than in G alone films, with main melting temperatures no significantly different for both blended films at around 55.8 °C and 55.4 °C respectively. Second scans (Traces G-L_{1000} and G-L_{2400}, dash lines) showed little variations in the corresponding lowest Tg data; the second glass transition process underwent however some complexity in the sense that two Tg values emerged, i.e., one at a lower and the other at a higher (more subtly) temperature than in the first scan: − 28.3 ± 0.7 °C plus – 11.9 ± 0.9 °C for G-L_{1000}, and − 20.7 ± 1.2 °C plus – 8.9 ± 0.9 °C for G-L_{2400}. The two sets of values for both blended G-L films were significantly different in their lower temperature components, but not significantly different in their higher temperature components. It is worth-noting that the first glass transition process at the lowest temperature range (Tg´s at roughly – 63 °C for G-L_{1000} and – 55 °C for G-L_{2400}) seemed similar to that observed in a previous work (Gómez-Estaca, Gómez-Guillén, Fernández-Martín & Montero, 2011) dealing with several composite films from fish gelatin plus chitosan plasticized with the same

498 glycerol plus sorbitol addition. We reported an average Tg of – 32.9 °C as a
499 representative value for all the composition range studied (Gómez-Estaca et al., 2011).
500 Huang et al. (2003) have also reported by DSC similar low temperature Tg values
501 (compositionally varying from − 70 to − 75 °C) in SPI-lignin films and, by
502 complementarily using dynamic mechanical thermal analysis (DMTA) (Tg values from −
503 66 to − 74 °C), ascribed this phenomenon to the α-relaxation process of the SPI side
504 segments in the system. It was followed by a second glass transition process which
505 showed some complexity in the sense that it consisted of two successive transitions
506 (Inset: Traces G-L_{1000} and G-L_{2400}, solid lines) at the significantly different Tg values of
507 – 23.1 ± 0.4 °C plus – 11.9 ± 0.9 °C for G-L_{1000}, and − 20.7 ± 1.2 °C plus – 8.9 ± 0.9 °C
508 for G-L_{2400}. Both Tg couple values were significantly lower than that single of G,
509 indicating the plasticization role of lignin (L_{1000} > L_{2400}), as well as an (initially) total
510 miscibility between both types of L and G at the proportions used in the blended films.
511 Corresponding melting endotherms were considerably and significantly smaller (with a
512 flatter trace: not significantly different values of 5.23 ± 0.25 J/g_{dm} for G-L_{1000} and 6.14 ±
513 0.16 J/g_{dm} for G-L_{2400}) than in G alone films, with main melting temperatures no
514 significantly different for both blended films at around 55.8 °C and 55.4 °C respectively.
515 The two sets of values for both blended G-L films were significantly different in their
516 lower temperature components, but not significantly different in their higher
517 temperature components. The Tg doublet presence could likely be due to the
518 appearance of a certain immiscibility between hydrophobic L and hydrophilic G leading
519 to a microphase separation, which provide more space for the G mobility. This
520 phenomenon has been reported by Huang et al. (2003) to occur in the SPI-lignin films,
521 and by Núñez-Flores et al. (2012) in (chemically near) fish gelatin plus lignosulphonate
522 films. The lower temperature component values of the respective Tg doublets
523 suggested that the above discussed immiscibility (microphase separation) enhanced
524 the initial plasticization effect of L_{1000} with respect to L_{2400}. The higher temperature
525 components were not significantly different but presented significant differences to the

526 Tg value of G, suggesting that immiscibility produced the segregation of a L-rich and a
527 L-pour phase respectively. Lignin is the common name of a family of wholly amorphous
528 aromatic polymers derived by oxidative condensation of phenolic precursors, very
529 branchy configured and containing several structural units which may yield very
530 complex structures. According to Guigo, Mija, Vincent & Sbirrazzouli (2009), glass
531 transition temperatures reported for isolated lignin in the literature cover a wide
532 temperature range, nearly between 80 and 200 ºC, mainly depending on differences in
533 molecular weight, delignification processes and vegetal origin of the product. It has
534 been speculated (Kubo & Kadla, 2005) that these high Tg temperatures are mostly
535 related to the low mobility of lignin chains highly constituted by aromatic units with
536 several polar groups, which facilitates the presence of different bond types, hydrogen-
537 bonding contributing significantly to that lignin segments mobility. Second scans
538 showed little variations in the glass transition processes (Inset: Traces G-L_{1000} and G-
539 L_{2400}, dash lines), practically restricted to a down shifting of around 2 – 3 °C in
540 corresponding Tg data. No remnant melting processes were detected.

541 When crystallization was carried out at 0 °C, film melting temperatures were recorded
542 at 52.8 ± 0.3 °C for G-L_{1000} and 51.0 ± 1.2 °C for G-L_{2400}, which were not significantly
543 different, nor to the G alone film. Corresponding melting enthalpies were not
544 significantly different, 4.78 ± 0.25 for G-L_{1000} and 5.14 ± 0.25 J/g_{dm} for G-L_{2400}, although
545 somewhat smaller (no significant) than those at subzero temperature conditioning, and
546 significantly lower than in the G alone film. The presence of lignin in the films seems to
547 restrict G from melting in a similar way irrespective of the lignin type in the blend. This
548 suggested that G apparently underwent a strong intermolecular interaction of similar
549 kind and extent with both types of lignin L_{1000} and L_{2400}, everything in main agreement
550 with above FTIR results. Second scans (not shown) yielded flat DSC traces indicating
551 that G underwent complete melting in the previous runs. On the other hand, it is
552 interesting to point out that the G-L films so conditioned (even more at room

553 temperature) are well above their corresponding glass transition temperatures, i.e.,
554 they are located at the rubbery state domain of the phase diagram. This could mean
555 that the above commented plasticization role of current lignin types may be not
556 prevalent any more, and water may likely play instead a relevant contribution to the
557 system plasticization and, consequently to the physical properties of these composite
558 films. Thus, as assessed by water activity and FTIR results, main differences in
559 mechanical properties and WVP between G-L_{1000} and G-L_{2400} films could be largely
560 attributed to a different film hydration level (G-L_{1000} < G-L_{2400}, with subsequently
561 paralleled plasticizing effects in opposition to those previously discussed at the glassy
562 state) rather than to a distinct effect of each lignin on protein conformation, especially
563 concerning triple helical structure. Comparison of current results was not possible due
564 to the absence of precedent literature data on G-L systems.

565

566 **Microstructure**

567 The freeze-fractured transversal section microstructure of gelatin and gelatin-lignin
568 films is shown in Fig. 5. The addition of lignin provoked a strong disruption of the
569 smooth and homogeneous structure of the parent gelatin film, inducing a partial
570 laminar-like appearance with decreased density, which tended to be more abrupt in the
571 G-L_{1000} film. This special feature did not apply to the whole section, but only to the side
572 which has been subjected to the water evaporation during drying process. Despite the
573 compatibility of lignin and gelatin denoted by the homogeneous appearance of the
574 corresponding film forming solutions, the bimodal microstructure in the composite films
575 would indicate some phase segregation of the two components, in accordance to the
576 above mentioned gelatin structural changes induced by lignin. Certain degree of
577 immiscibility between hydrophobic groups of lignin and hydrophilic groups in SPI has

been shown to prevent interaction among SPI molecules causing microphase separation in the corresponding blends (Huang et al., 2003).

Antioxidant properties

The water soluble fraction of gelatin and gelatin-lignin films was studied for its antioxidant capacity. Table 4 shows the radical scavenging capacity (ABTS assay) and the ferric ion reducing power (FRAP assay) of gelatin and gelatin-lignin films, which had been solubilized in water for 16 hours. The presence of lignin increased significantly ($p<0.05$) the antioxidant properties of the composite films, especially in the case of the G-L_{1000} film, despite its decreased water solubility (Table 1). The gelatin-lignin films registered ABTS and FRAP values comparable to that achieved in fish gelatin films enriched with an antioxidant borage extract (Gómez-Estaca, Giménez, Montero & Gómez-Guillén, 2009). This property could be useful for preservation of certain types of food in which oxidation process may represent a limiting factor determining its self-life. To this regard, a similar fish gelatin-lignin (G-L_{1000}) film was reported to reduce the levels of protein carbonyl groups formed in Atlantic salmon muscle immediately after high-pressure processing, and prevented lipid oxidation from taking place at advanced stages of chilled storage (Ojagh et al., 2011).

In the present study, composite gelatin films with lignin L_{1000} were found to present considerably higher radical scavenging and Fe reducing capacities than those with lignin L_{2400}. Moreover, the mechanical and water resistance of gelatin-lignin blend films were also higher with L_{1000} than with L_{2400}. For this reason L_{1000} was subjected to a study of functional properties, concerning antioxidant, antimicrobial and cytotoxic properties, in order to determine its potential in food packaging applications.

603 **Functional properties of lignin**

604 The noticeable antioxidant capacity of gelatin-lignin films is strongly related to the high
605 antioxidant properties of lignin. The DPPH radical scavenging capacity of L_{1000} and
606 Trolox, expressed as IC_{50} values, are shown in Table 5. When compared with Trolox,
607 L_{1000} showed significantly lower antioxidant activity, with IC_{50} values approximately 2-
608 fold higher than those obtained for Trolox. The radical scavenging activity of L_{1000},
609 however, was about 3-fold higher than the activity of several lignosulphonates reported
610 by Nuñez-Flores et al. (2012).

611 Given the potential application of lignin as active packaging material in contact with
612 food, it is of great interest to study its possible cytotoxic effects. The cytotoxic effect of
613 L_{1000} on fibroblast 3T3 cells is shown in Table 5. The IC_{50} value obtained for L_{1000}
614 (631±92 μg/ml) reveals that this compound has cytotoxic effects, but only at very high
615 concentrations. In our study, L_{1000} showed IC_{50} values similar to those reported for
616 Curan 100 (Lignotech) or Bagase (Granit) lignins (600-650 μg/ml) on 3T3 cell line after
617 24 h of exposure (Ugartondo et al., 2008), but lower to those reported for several
618 lignosulphonates (IC_{50} ~ 1200 μg/ml, Ugartondo et al., 2008; IC_{50} 1200 ~ 1700 μg/ml,
619 Nuñez-Flores et al., 2012). When the cytotoxic potential of L_{1000} was related to its
620 antioxidant activity, it could be observed that the effective antioxidant concentration
621 was noticeably smaller than the cytotoxic one (about 17-fold lower), so this compound
622 could be considered antioxidant at non-cytotoxic concentrations.

623 The lignin L_{1000} showed no antimicrobial activity against the 26 microbial strains studied
624 (data not shown). The pH of lignin (in our assay lignin was tested at neutral and basic
625 pH) could be partly responsible for this lack of activity, although the antimicrobial
626 effectiveness of polyphenolic compounds from other sources (green tea) was similar in
627 a pH range of 4.0-7.0 (von Staszewski et al., 2011). Some authors suggested that the
628 inhibition of microbial growth by phenolic acids, among which includes the p-coumaric,

629 increased with decreasing pH (Wen at al., 2003). In our work no relationship was found
630 between antioxidant and antimicrobial properties of lignin, in contrast to the work of
631 Dizhbite et al. (2004), who assumed the connection between the antibacterial effect
632 and the scavenging activity of the kraft lignin soluble fraction.
633

634 **Conclusions**

635 Lignin represents an important waste material which could be successfully employed
636 as an active food packaging agent for providing fish gelatin films with antioxidant
637 capacity at non-cytotoxic concentrations. At the macroscopic level, lignin provided
638 adequate miscibility with gelatin, reducing the typical transparent appearance and
639 conferring a dark brownish color to gelatin films, without losing their visual
640 homogeneity. The structural analyses, however, revealed that lignin prevented the
641 interaction among gelatin molecules producing a certain microphase separation
642 between both components. Although the composite films were considerably more
643 plasticized than the single gelatin films, the water solubility was scarcely affected,
644 largely because the gelatin used (from warm water fish species) produced films with
645 reasonable low solubility.
646

647 **Acknowledgments**

648 This research was financed by the Spanish Ministerio de Ciencia e Innovación under
649 project AGL2008-00231/ALI. Author R. Núñez-Flores wish to thank for the concession
650 of a FPI grant.
651

652 LITERATURE CITED

653 Arvanitoyannis, I.S. (2002). Formation and properties of collagen and gelatin films and
654 coatings. Ch.11. In A. Gennadios (Ed.), Protein-based Films and Coatings (pp. 275-
655 304). Boca Ratón, Florida: CRC Press.

656 Avena-Bustillos, R.J., Olsen, C.W., Olson, D.A., Chiou, B., Yee, E., Bechtel, P.J., &
657 McHugh, T.H. (2006). Water vapor permeability of mammalian and fish gelatin films.
658 *Journal of Food Science*, 71(4), E202-E207.

659 Badii, F., & Howell, N. K. (2006). Fish gelatin: structure, gelling properties and
660 interaction with egg albumen proteins. Food Hydrocolloids, 20, 630-640.

661 Ban, W., Song, J., & Lucia, L.A. (2007). Influence of natural biomaterials on the
662 absorbency and transparency of starch-derived films: An optimization study. *Industrial*
663 *and Engineering Chemistry Research*, 46(20), 6480-6485.

664 Baumberger, S., Lapierre, C., Monties, B., Lourdin, D., & Colonna, P. (1997).
665 Preparation and properties of thermally moulded and cast lignosulfonates-starch
666 blends. *Industrial Crops and Products*, 6(3-4), 253-258.

667 Bergo, P., Sobral, P.J.A. (2007). Effects of plasticizer on physical properties of pigskin
668 gelatin films. *Food Hydrocolloids*, 21(8), 1285-1289.

669 Brand-Williams, W., Cuvelier, M. E., & Berset, C. (1995). Use of free radical method to
670 evaluate antioxidant activity. *Lebensmittel-Wissenschaft und Technologic*, 28, 25–30.

671 Cao, N., Fu, Y., & He, J. (2007). Preparation and physical properties of soy protein
672 isolate and gelatin composite films. *Food Hydrocolloids*, 21(7), 1153-1162.

673 Carvalho, R.A., Sobral, P.J.A., Thomazine, M., Habitante, A.M.Q.B., Giménez, B.,
674 Gómez-Guillén, M.C. & Montero, P. (2008). Development of edible films based on
675 differently processed Atlantic halibut (*Hippoglossus hippoglossus*) skin gelatin. *Food*
676 *Hydrocolloids*, 22(6), 1117-1123.

677 Chiellini, E., Cinelli, P., Fernandes, E.G., Kenawy, E.-R.S., & Lazzeri, A. (2001).
678 Gelatin-based blends and composites. Morphological and thermal mechanical
679 characterization. *Biomacromolecules*, 2(3), 806-811.

680 Cruz JM, Domínguez JM, Domínguez H, Parajó JC. 2001. Antioxidant and
681 antimicrobial effects of extract from hydrolysates of lignocellulosic materials. *Journal of*
682 *Agricultural and Food Chemistry*, 49:2459-2464.

683 Cui, G., Xia, W., Chen, G., Wei, M., & Huang, J. (2007). Enhanced mechanical
684 performances of waterborne polyurethane loaded with lignosulfonate and its
685 supramolecular complexes. *Journal of Applied Polymer Science*, 106(6), 4257-4263.

686 Cuq, B., Gontard, N., Cuq, J., & Guilbert, S. (1997). Selected Functional Properties of
687 Fish Myofibrillar Protein-Based Films As Affected by Hydrophilic Plasticizers. *Journal of*
688 *Agricultural and Food Chemistry*, 45(3), 622-626.

689 Dizhbite, T., Telysheva, G., Jurkjane, V., & Viesturs, U. (2004). Characterization of the
690 radical scavenging activity of lignins-natural antioxidants. *Bioresource Technology*, 95,
691 309–317.

692 Dong, X., Dong, M., Lu, Y., Turley, A., Jin, T., & Wu, C. (2011). Antimicrobial and
693 antioxidant activities of lignin from residue of corn stover to ethanol production.
694 *Industrial Crops and Products*, 34, 1629-1634.

695 Feldman, D., Lacasse, M., & Beznaczuk, L.M. (1986). Lignin-polymer systems and
696 some applications. *Progress in Polymer Science*, 12(4), 271-276.

697 Fernandes, D.M., Winkler Hechenleitner, A.A., Job, A.E., Radovanocic, E., & Pineda,
698 E.A.G. (2006). Thermal and photochemical stability of poly(vinyl alcohol)/modified lignin
699 blends. *Polymer Degradation and Stability*, 91(5), 1192-1201.

700 Fukumoto, L. R., & Mazza, G. (2000). Assessing antioxidant and prooxidant activities
701 of phenolic compounds. *Journal of Agriculture and Food Chemistry*, 48, 3597–3604.

Gómez-Estaca, J., Gómez-Guillén, M. C., Fernández-Martín, F., & Montero, M. P. (2011). Effects of gelatin origin, bovine-hide and tuna-skin, on the properties of compound gelatin-chitosan films. *Food Hydrocolloids*, 25, 1461-1469.

Gómez-Estaca, J., Giménez, B., Montero, P., & Gómez-Guillén, M.C. (2009). Incorporation of antioxidant borage extract into edible films based on sole skin gelatin or a commercial fish gelatin. *Journal of Food Engineering*, 92(1), 78-85.

Gómez-Estaca, J., Montero, P., Fernández-Martín, F., & Gómez-Guillén, M.C. (2009). Physico-chemical and film-forming properties of bovine-hide and tuna-skin gelatin: A comparative study. *Journal of Food Engineering*, 90(4), 480-486.

Gómez-Guillén, M.C., Ihl, M., Bifani, V., Silva, A., & Montero, P. (2007). Edible films made from tuna-fish gelatin with antioxidant extracts of two different murta ecotypes leaves (*Ugni molinae* Turcz). *Food Hydrocolloids*, 21(7), 1133-1143.

Guigo, N., Mija, A., Vincent, L., & Sbirrazzouli, N. (2009). Molecular mobility and relaxation process of isolated lignin studied by multifrequency calorimetric experiments. *Physical Chemistry Chemical Physics*, 11, 1227-1236.

Hoque, M.S., Benjakul, S., Prodpran, T. (2011). Effects of partial hydrolysis and plasticizer content on the properties of film from cuttlefish (*Sepia pharaonis*) skin gelatin. *Food Hydrocolloids*, 25 (1), 82-90.

Huang, J., Zhang, L., & Chen, F. (2003). Effects of lignin as a filler on properties of soy protein plastics. I. Lignosulfonate. *Journal of Applied Polymer Science,* 88(14), 3284-3290.

Jongjareonrak, A., Benjakul, S., Visessanguan, W., Prodpran, T., & Tanaka, M. (2006). Characterization of edible films from skin gelatin of brownstripe red snapper and bigeye snapper. *Food Hydrocolloids*, 20(4), 492-501.

726 Jongjareonrak, A., Benjakul, S., Visessanguan, W., Tanaka, M. 2008. Antioxidative
727 activity and properties of fish skin gelatin films incorporated with BHT and α-tocopherol.
728 *Food Hydrocolloids*, 22(3), 449-458.

729 Julinová, M., Kupec, J., Alexy, P., Hoffmann, J., Sedlařík, V., Vojtek, T., Chromčáková,
730 J., & Bugaj, P. (2010). Lignin and starch as potential inductors for biodegradation of
731 films based on poly(vinyl alcohol) and protein hydrolysate. *Polymer Degradation and*
732 *Stability*, 95(2), 225-233.

733 Kadla, J.F., & Kubo, S. (2003). Miscibility and hydrogen bonding in blends of
734 poly(ethylene oxide) and kraft lignin. *Macromolecules*, 36(20), 7803-7811.

735 Kubo, S. & Kadla, J. F. (2005). Hydrogen bonding in lignin: A model compound study.
736 *Biomacromolecules*, 6, 2815-2821.
737 Kosikova B., Demianova, V., & Kakurakova, M. (1993). Sulfur-free lignins as
738 composites of polypropylene films. *Journal of Applied Polymer Science*, 47, 1065–
739 1073.

740 Li, Y., & Sarkanen, S. (2002). Alkylated kraft lignin-based thermoplastic blends with
741 aliphatic polyesters. *Macromolecules,* 35(27), 9707-9715.

742 Lu, F.J., Chu, L.H., & Gau, R.J. (1998). Free radical-scavenging properties of lignin.
743 *Nutrition and Cancer*, 30(1), 31-38.

744 Mishra, S.B., Mishra, A.K., Kaushik, N.K., & Khan, M.A. (2007). Study of performance
745 properties of lignin-based polyblends with polyvinyl chloride. *Journal of Materials*
746 *Processing Technology*, 183(2-3), 273-276.

747 Moraes, I.C.F., Carvalho, R.A., Bittante, A.M.Q.B., Solorza-Feria, J., & Sobral, P.J.A.
748 (2009). Film forming solutions based on gelatin and poly(vinyl alcohol) blends: Thermal
749 and rheological characterizations. *Journal of Food Engineering*, 95(4), 588-596.
750

751 Núñez-Flores, R., Giménez, B., Fernández-Martín, F., López-Caballero, M.E., Montero,
752 M.P., & Gómez-Guillén, M.C. (2012). Role of lignosulphonate in properties of fish
753 gelatin films. *Food Hydrocolloids*, 27, 60-71.

754 Oh-Hara T., Sakagami H, Kawazoe Y, Kaiya t, Komatsu N, Ohsawa N, Fujimaki M,
755 Tanuma SI, Konno K. 1990. Antimicrobial spectrum of lignin-related pine cone extracts
756 of Pinus Parviflora Sieb. Et Zucc. In vivo 4:7-12.
757

758 Ojagh, S.M., Núñez-Flores, R., López-Caballero, M.E., Montero, M.P., & Gómez-
759 Guillén, M.C. (2011). Lessening of high-pressure-induced changes in Atlantic salmon
760 muscle by the combined use of a fish gelatin-lignin film. *Food Chemistry*, 125(2), 595-
761 606.

762 Pan, X., Kadla, J.F., Ehara, K., Gilkes, N., & Saddler, J.N. (2006). Organosolv ethanol
763 lignin from hybrid poplar as a radical scavenger: relationship between lignin structure,
764 extraction conditions, and antioxidant activity. *Journal of Agriculture and Food*
765 *Chemistry,* 54, 5806–5813.

766 Payne, K. J., & Veis, A. (1988). Fourier transform IR spectroscopy of collagen and
767 gelatin solutions: Deconvolution of the amide I band for conformational studies.
768 *Biopolymers*, 27(11), 1749-1760.

769 Pereira, A.A., Martins, G.F., Antunes, P.A., Conrrado, R., Pasquini, D., Job, A.E.,
770 Curvelo, A.A.S., & Constantino, C.J.L. (2007). Lignin from sugar cane bagasse:
771 Extraction, fabrication of nanostructured films, and application. *Langmuir*, 23(12), 6652-
772 6659.

773 Pérez-Mateos, M., Montero, P., & Gómez-Guillén, M.C. (2009). Formulation and
774 stability of biodegradable films made from cod gelatin and sunflower oil blends. *Food*
775 *Hydrocolloids*, 22(4), 53-61.

776 Prystupa, D. A., & Donald, A. M. (1996). Infrared study of gelatin conformations in the
777 gel and sol states. *Polymer Gels and Networks*, 4(2), 87-110.

778 Rahmann, M. S., Al-Saidi, G. S., & Guizani, N. (2008). Thermal characterization of
779 gelatin extracted from yellowfin tuna skin and commercial mammalian gelatin. *Food*
780 *Chemistry*, 108, 472-481.
781 Rohella, R.S., Sahoo, N., Paul, S.C., Choudhury, S., & Chakravortty, V. (1996).
782 Thermal studies on isolated and purified lignin. *Thermochimica Acta*, 287(1), 131-138.

783 Sakagami, H., Hashimoto, K., Suzuki, F., Ogiwara, T., Satoh, K., ito, H., Hatano, T.,
784 Takashi, Y., & Fujisawa, S. (2005). Molecular requirements of lignin-carbohydrate
785 complexes for expression of unique biological activities. *Phytochemistry*, 66, 2108-
786 2120.

787 Satoh, K., Kihara, T., Ida, Y., Sakagami, H., Koyama, N., Premanathan, M., Arakaki,
788 R., Nakashima, H., Komatsu, N., Fujimaki, M., Misawa, Y., Hata, N. (1999). Radical
789 modulation activity of pine cone extracts of *Pinus elliottii* var. elliottii. *Anticancer*
790 *Research*, 19, 357–364.

791 Sobral, P.J.A., Menegalli, F.C., Hubinger, M.D., & Roques, M.A. (2001). Mechanical
792 water vapor barrier and thermal properties of gelatin based edible films. Food
793 Hydrocolloids, 15 (4-6), 423-432.

794 Spiridon, I., Teaca, C.A., Bodirlau, R. (2011). Preparation and characterization of adipic
795 acid-modified starch microparticles/plasticized starch composite films reinforced by
796 lignin. *Journal of Material Science*, 46, 3241-3251.
797 Surewicz, W.K., & Mantsch, H.H. (1988). New insight into protein secondary structure
798 from resolution-enhanced infrared spectra. *Biochimica et Biophysica Acta - Protein*
799 *Structure and Molecular Enzymology*, 952(2), 115-130.

800 Ugartondo, V., Mitjans, M., & Vinardell, M.P. (2008). Comparative antioxidant and
801 cytotoxic effects of lignins from different sources. *Bioresource Technology*, 99(14),
802 6683-6687.

803 Vengal, J.C., & Srikumar, M. (2005). Processing and study of novel lignin-starch and
804 lignin-gelatin biodegradable polymeric films. *Trends in Biomaterials and Artificial*
805 *Organs*, 18(2), 237-241.

806 von Staszewski, M., Pilosof, A.M.R., Jagus, R.J. (2011). Antioxidant and antimicrobial
807 performance of different Argentinean green tea varieties as affected by whey proteins.
808 *Food Chemistry*, 125(1), 186-192.

809 Wen, A., Delaquis, P., Stanich, K., Toivonen, P. (2003). Antilisterial activity of selected
810 phenolic acids. *Food Microbiology*, 20(3), 305-311.

811 Wu, R.-L., Wang, X.-L., Li, F., Li, H.-Z., & Wang, Y.-Z. (2009). Green composite films
812 prepared from cellulose, starch and lignin in room-temperature ionic liquid. *Bioresource*
813 *Technology*, 100(9), 2569-2574.

814 Yakimets, I., Wellner, N., Smith, A. C., Wilson, R. H., Farhat, I., & Mitchell, J. (2005).
815 Mechanical properties with respect to water content of gelatin films in glassy state.
816 *Polymer*, 46(26), 12577-12585.

817 Zhang,S., Wang,Y., Herring,J.L., & Oh, J.-H. (2007). Characterization of edible film
818 fabricated with channel catfish (*Ictalurus punctatus*) gelatin extract using selected
819 pretreatment methods. *Journal of Food Science*, 72(9), 498-503.

820

LEGEND TO FIGURES

FIGURE 1.- Changes in light absorbance at wavelengths ranging from 250 to 700 nm of films based on mixtures of fish gelatin (G) and lignin (L_{1000} and L_{2400}) at the ratio 85% gelatin: 15% lignin (w/w). Single gelatin film, G; Compound films with lignin, G-L_{1000} and G-L_{2400}.

FIGURE 2.- ATR-FTIR spectra of films based on mixtures of fish gelatin (G) and lignin (L_{1000} and L_{2400}) at the ratio 85% gelatin: 15% lignin (w/w). Single gelatin film, G; Compound films with lignin, G-L_{1000} and G-L_{2400}.

FIGURE 3.- Second derivative of amide A band from FTIR spectra of films based on mixtures of fish gelatin (G) and lignin (L_{1000} and L_{2400}) at the ratio 85% gelatin: 15% lignin (w/w). Single gelatin film, G; Compound films with lignin, G-L_{1000} and G-L_{2400}.

FIGURE 4.- Normalized typical DSC traces (Heat flow, W/g_{dm}, vs.Temperature, °C) of films based on mixtures of fish gelatin (G) and lignin (L1000 and L2400) at the ratio 85% gelatin: 15% lignin (w/w). Single gelatin film, G; Compound films with lignin, G-L_{1000} and G-L_{2400}. First scans in conditioned films at − 80 °C, Solid lines; Second scans, Dash lines. First scans in conditioned films at 0 °C, Dot lines. Arrows roughly indicate Tg locations: Inset shows DSC traces of blended films magnified in the temperature zone of the complex glass transition processes. Solid, First scans; Dash, Second scans. Bar indicates the ordinate scale (0.5 W/g_{dm}).

845 FIGURE 5.- Scanning electron microscopy at low temperature (Cryo-scanning) of films
846 based on mixtures of fish gelatin (G) and lignin (L_{1000} and L_{2400}) at the ratio 85% gelatin:
847 15% lignin (w/w). Single gelatin film, G; Compound films with lignin, G-L_{1000} and G-
848 L_{2400}.

849

Table 1.- Physical properties of films based on mixtures of fish gelatin (G) and lignin (L_{1000} and L_{2400}) at the ratio 85% gelatin: 15% lignin (w/w).

Gelatin-Lignin	Thickness (mm)	Aw	TS $x10^6$ (N/m^2)	EAB (%)	BF (N)	BD (%)	WATER SOLUBILITY (%)	WVP $x10^{-8}$ ($g.mm/h.Pa.cm^2$)
G	0.096±0.01[a]	0.375[a]	16.44±0.18[a]	136.6±39.8[a]	26.08±0.25[a]	15.85±4.33[a]	44.29±0.97[a]	2.06±0.10[a]
G-L_{1000}	0.124±0.02[a]	0.390[b]	12.13±0.48[b]	316.48±19.7[b]	18.95±1.43[b]	54.90±0.13[b]	39.38±1.73[b]	2.17±0.54[a]
G-L_{2400}	0.100±0.02[a]	0.467[c]	7.51±0.05[c]	362.83±39.6[b]	16.38±2.05[b]	65.70±1.16[c]	46.52±1.66[a]	4.58±0.53[b]

Aw: water activity; TS: tensile strength; EAB: elongation at break; BF: breaking force; BD: breaking deformation; WVP: water vapour permeability.

Different letters *a,b,c* in the same column indicate significant differences ($p<0.05$) among samples.

Table 2.- Color parameters and transparency level of films based on mixtures of fish gelatin (G) and lignin (L_{1000} and L_{2400}) at the ratio 85% gelatin: 15% lignin (w/w).

Gelatin-Lignin	L*	a*	b*	Opacity Abs_{600}/mm
G	34.04 ± 0.47^{a}	-0.55 ± 0.04^{a}	-0.89 ± 0.02^{a}	0.52±0.00
G-L_{1000}	25.05 ± 0.36^{b}	0.46 ± 0.02^{b}	-0.37 ± 0.09^{b}	9.84±2.09
G-L_{2400}	25.84 ± 0.18^{c}	1.98 ± 0.18^{c}	1.05 ± 0.19^{c}	4.62±.0.33

Different letters *a,b,c* in the same column indicate significant differences ($p<0.05$) among samples.

Table 3.- Viscoelastic properties of film forming solutions based on mixtures of fish gelatin (G) and lignin (L_{1000} and L_{2400}) at the ratio 85% gelatin: 15% lignin (w/w).

Gelatin-Lignin	$G'_{5°C}$ (Pa)	$G''_{5°C}$ (Pa)	$p.a._{5°C}$ (°)	Tg (°C)	Tm (°C)
G	852±25	11.30±0.23	0.91±0.01	15	26
G-L_{1000}	1.65±0.05	1.81±0.05	40.55±2.03	6	18
G-L_{2400}	10.10±0.30	2.25±0.09	12.70±0.25	7	18

p.a.: phase angle
Tg: gelling temperature
Tm: melting temperature

Table 4.- Radical scavenging and Fe ion reducing capacities of films based on mixtures of fish gelatin (G) and lignin (L_{1000} and L_{2400}) at the ratio 85% gelatin: 15% lignin (w/w).

Gelatin-Lignin	ABTS (mg vit C/g film)	FRAP (μmol Fe^{2+}/g film)
G	6.54±0.13[a]	8.60±0.60[a]
G-L_{1000}	27.82±2.19[b]	258.97±8.83[b]
G-L_{2400}	15.31±0.88[c]	180.20±5.71[c]

Different letters *a,b,c* in the same column indicate significant differences ($p<0.05$) among samples.

Table 5. Radical scavenging efficacy and cytotoxic effect of L_{1000}

	DPPH IC_{50} (μg/ml)	**Cytotoxicity IC_{50} (μg/ml)**
L_{1000}	36.5 ± 5.5^{b}	631 ± 92
Trolox	$15.7 \pm 0,2^{a}$	

Different letters *a,b* in the same column indicate significant differences ($p<0.05$) among samples.

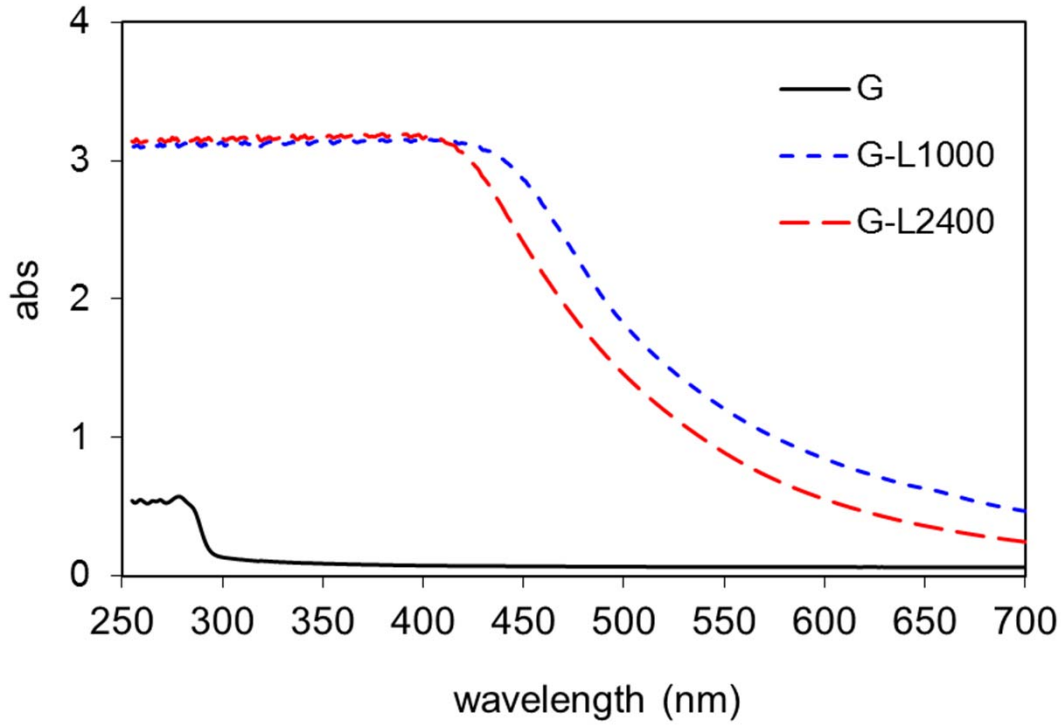
4
3
2
1
0
abs
G
G-L1000
G-L2400
250
300
350
400
450
500
550
600
650
700
wavelength (nm)

FIG. 1

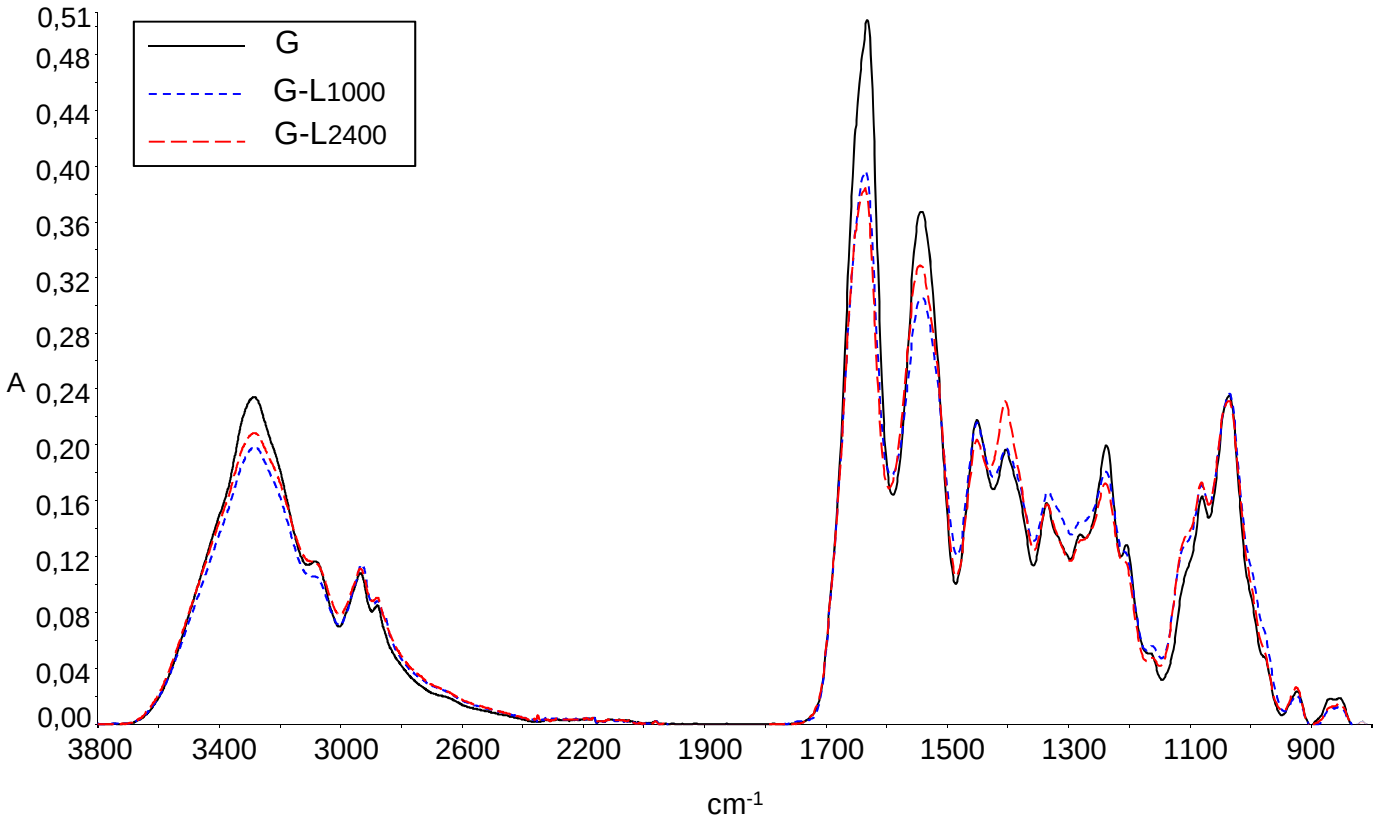
G
G-L1000
G-L2400
A
0,51
0,48
0,44
0,40
0,36
0,32
0,28
0,24
0,20
0,16
0,12
0,08
0,04
0,00
3800
3400
3000
2600
2200
1900
1700
1500
1300
1100
900
cm-1

FIG. 2

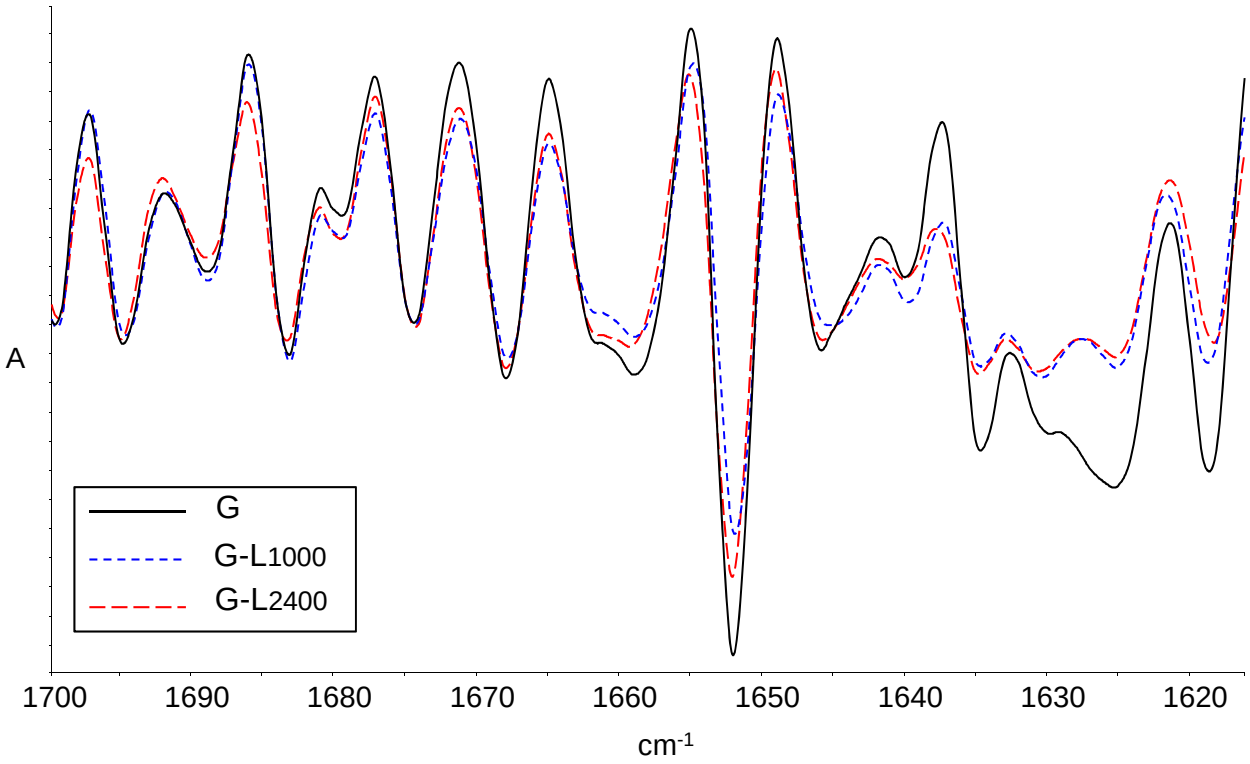
A
G
G-L1000
G-L2400
1700
1690
1680
1670
1660
1650
1640
1630
1620
cm-1

FIG. 3

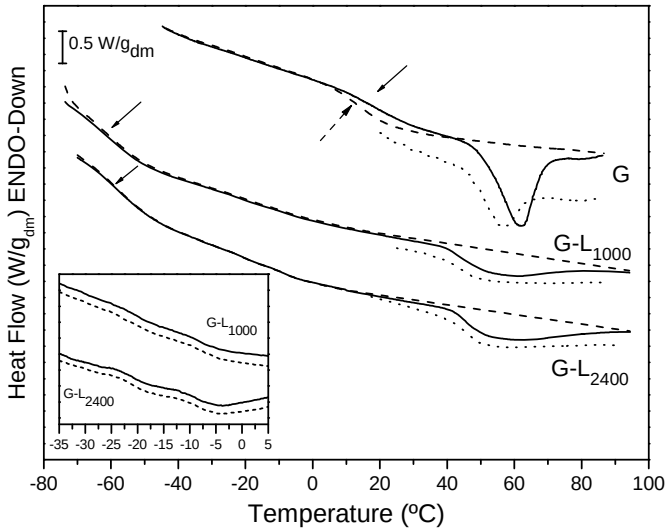
0.5 W/g$_{dm}$
Heat Flow (W/g$_{dm}$) ENDO-Down
G
G-L$_{1000}$
G-L$_{2400}$
G-L$_{1000}$
G-L$_{2400}$
-35 -30 -25 -20 -15 -10 -5 0 5
-80 -60 -40 -20 0 20 40 60 80 100
Temperature (ºC)

FIG. 4

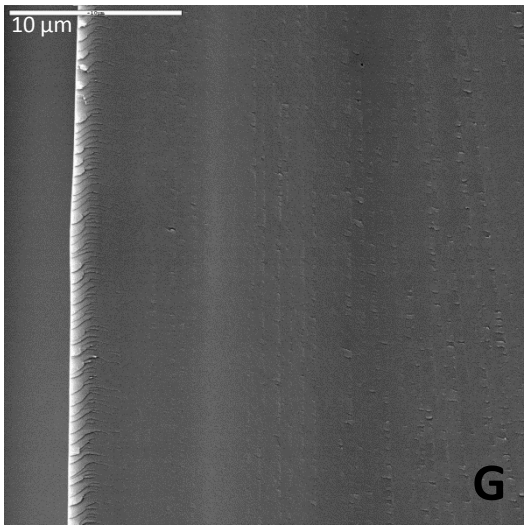

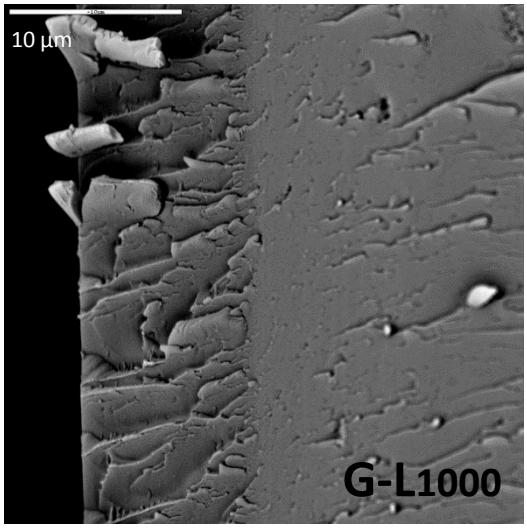

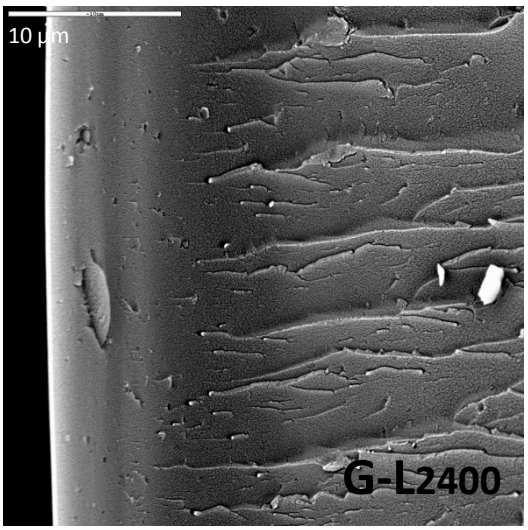

FIG. 5